Обзор ArXiv: astro-ph, 17-28 августа 2020

От Сильченко О.К.

ArXiv: 2008.08092

CGM^2 I: The Extent of the Circumgalactic Medium Traced by Neutral Hydrogen

Matthew C. Wilde,[1] Jessica K. Werk,[1] Joseph N. Burchett,[2,3] J. Xavier Prochaska,[2,4] Kirill Tchernyshyov,[1] Todd M. Tripp,[5] Nicolas Tejos,[6] Nicolas Lehner,[7] Rongmon Bordoloi,[8] John M. O'Meara,[9] and Jason Tumlinson[10]

[1] *University of Washington, Department of Astronomy, Seattle, WA 98195, USA*
[2] *University of California, Santa Cruz; 1156 High St., Santa Cruz, CA 95064, USA*
[3] *Department of Astronomy , New Mexico State University, PO Box 30001, MSC 4500, Las Cruces, NM 88001*
[4] *Kavli Institute for the Physics and Mathematics of the Universe (Kavli IPMU) The University of Tokyo; 5-1-5 Kashiwanoha, Kashiwa, 277-8583, Japan*
[5] *Department of Astronomy, University of Massachusetts, 710 North Pleasant Street, Amherst, MA 01003-9305, USA*
[6] *Instituto de Física, Pontificia Universidad Católica de Valparaíso, Casilla 4059, Valparaíso, Chile*
[7] *Department of Physics, University of Notre Dame, Notre Dame, IN 46556*
[8] *North Carolina State University, Department of Physics, Raleigh, NC 27695-8202*
[9] *W. M. Keck Observatory, 65-1120 Mamalahoa Hwy., Kamuela, HI 96743, USA*
[10] *Space Telescope Science Institute, Baltimore, MD, USA*

ABSTRACT

We present initial results from the *COS and Gemini Mapping the Circumgalactic Medium* (CGMCGM $\equiv$ CGM^2) survey. The CGM^2 spectroscopic survey consists of 1689 galaxies, all with high-quality Gemini GMOS spectra suitable for precise redshift measurements, within 1 Mpc of twenty-two $z \lesssim 1$ quasars, all with existing S/N$\sim$10 HST-COS G130M+G160M spectra. We show that the H I covering fraction above a threshold of $N_{\rm HI} > 10^{14}{\rm cm}^{-2}$ is $\gtrsim 0.6$ within 1.5 virial radii ($R_{\rm vir} \sim R_{200m}$) of galaxies having stellar masses $10^8 M_\odot < M_\star < 10^{11} M_\odot$. We examine the kinematics of the H I

Пример поля – а всего их 22

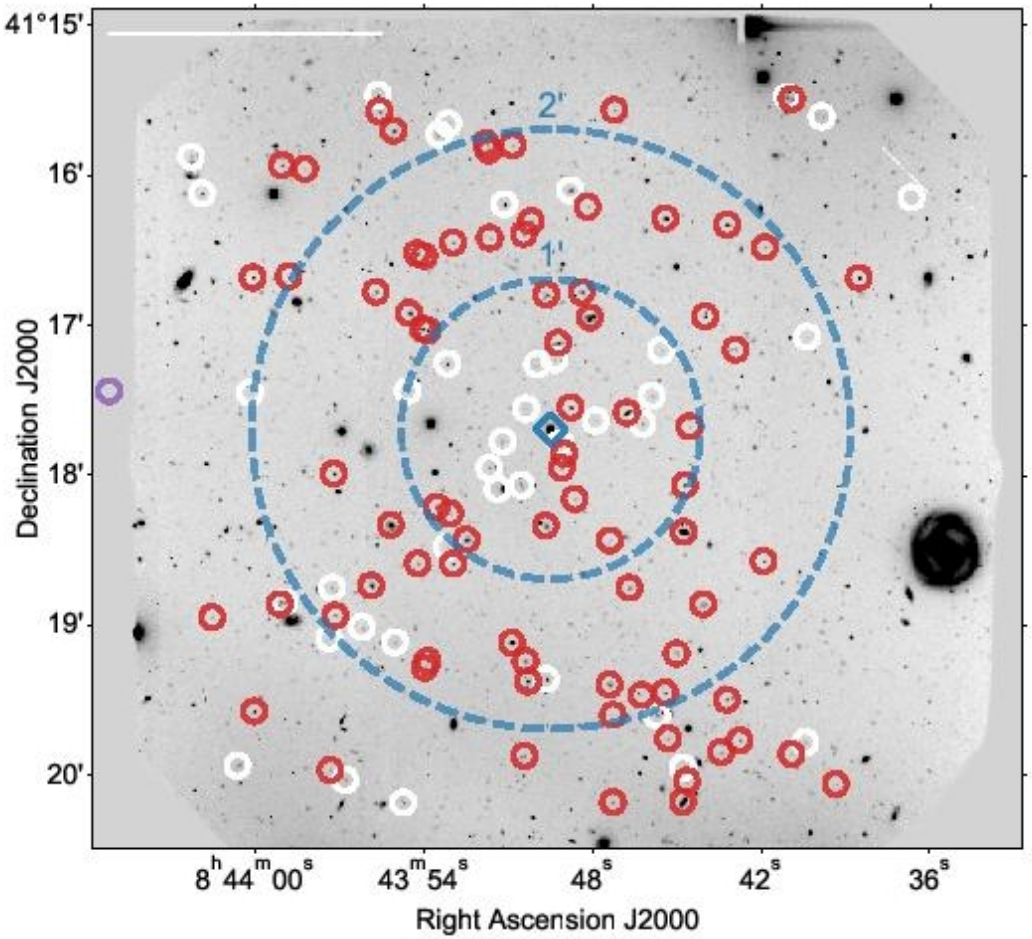

В синем ромбе - квазар

Распределение галактик по красным смещениям

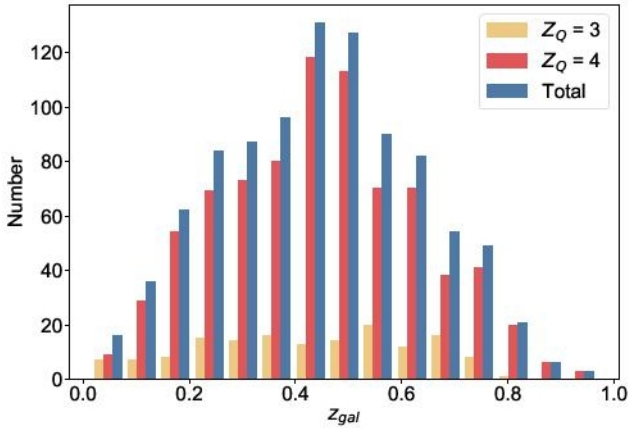

Figure 2. The redshift distribution of the CGM^2 galaxy catalog for galaxies with $z < z_{\rm QSO}$. The redshift reliability is encoded in yellow and red. Red represents our most reliable redshift quality flag of '4' with spectra displaying more than one strong absorption or emission line. A quality flag of '3' was reserved for spectra with only one strong emission line and thus a less reliable redshift designation. Approximately 85% (801 out of 953) of our spectra were given the highest reliability flag. The typical statistical uncertainly of our redshifts is $\sigma_z \sim$ 50-100 km s^{-1} ($z \simeq$ 0.00016-0.00030).

Отрезали по z<0,48

Примеры спектров GEMINI –для красных смещений сойдет

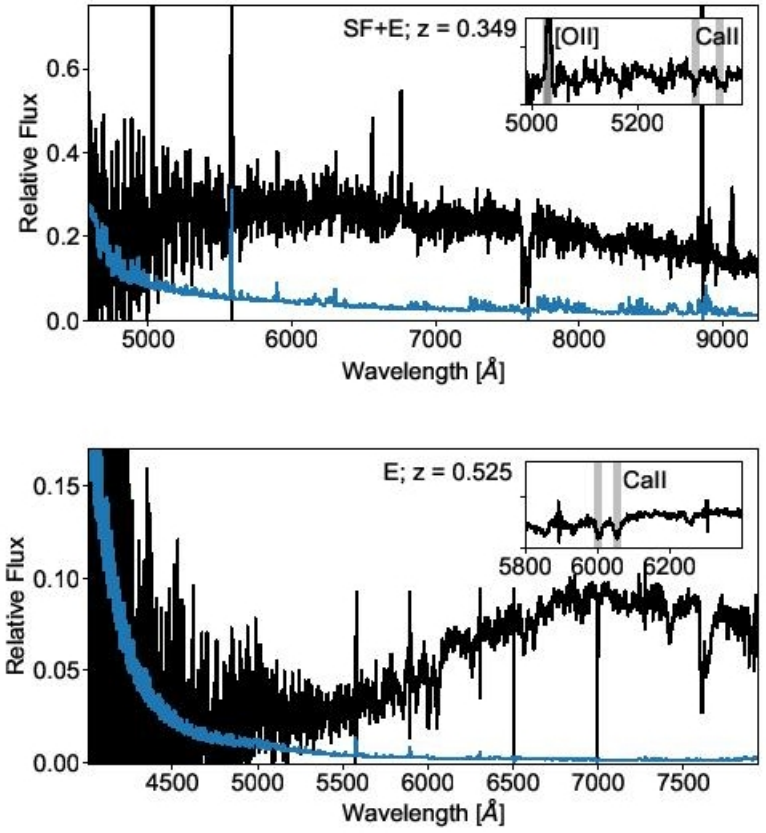

Figure 3. Examples of typical Gemini-GMOS spectra with a quality flag of $Z_Q = 4$, along with the error shown in blue.

Галактики – всякие и разные

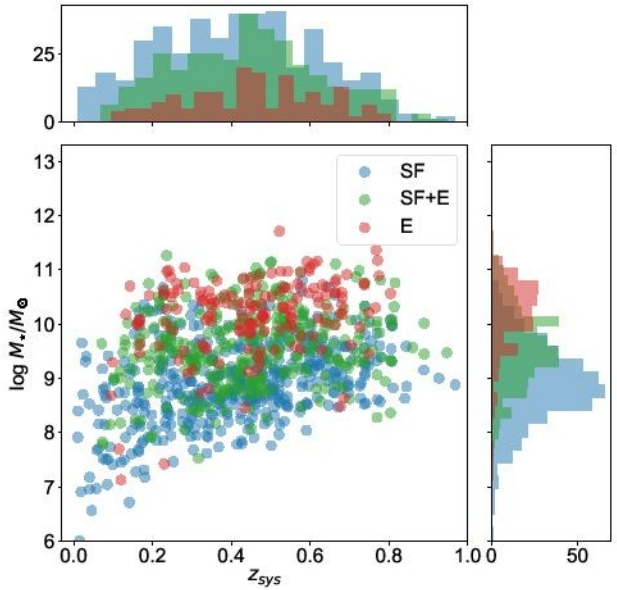

Figure 5. The distribution of galaxy stellar mass as a function of galaxy systemic redshift with marginal distributions on the right and top. The red, green, blue colors correspond to the galaxy spectral type determined from visual

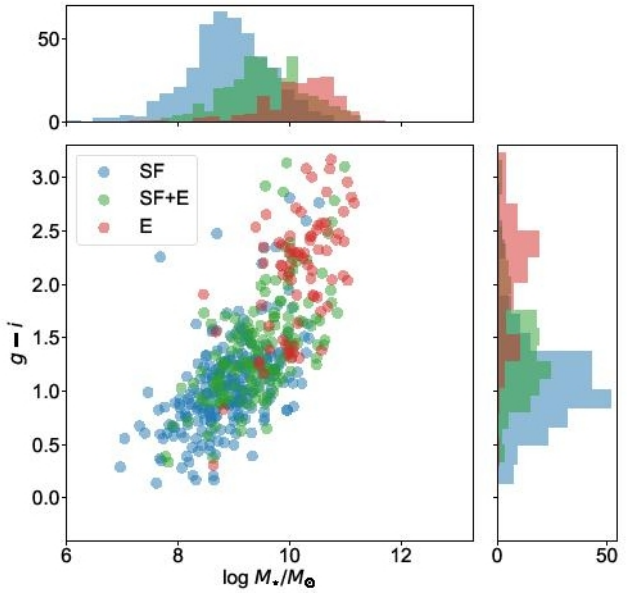

Figure 6. CGM^2 sample in a color-magnitude diagram using the $g - r$ color and the galaxy stellar mass, $M_\star$. Multiband photometry was not available for all of the galaxy targets, only objects with both bands are shown here. The bi-

А это системы водородных линий в спектрах квазаров

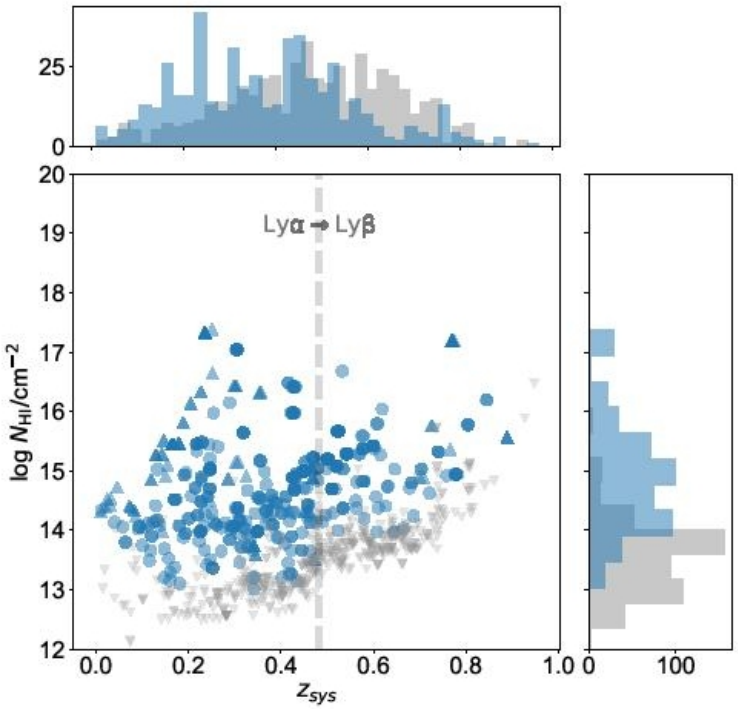

Figure 7. Scatter plot and marginal distributions of column densities vs. redshift for the H I systems detected in the CGM^2 survey. The mean 1σ uncertainties on column density is 0.17 dex for unsaturated H I lines to column densities $\simeq 10^{17.5}$ cm^{-2}, which is of order the size of the symbol (see Fig-

Статистика плотностей газа и частоты встречаемости

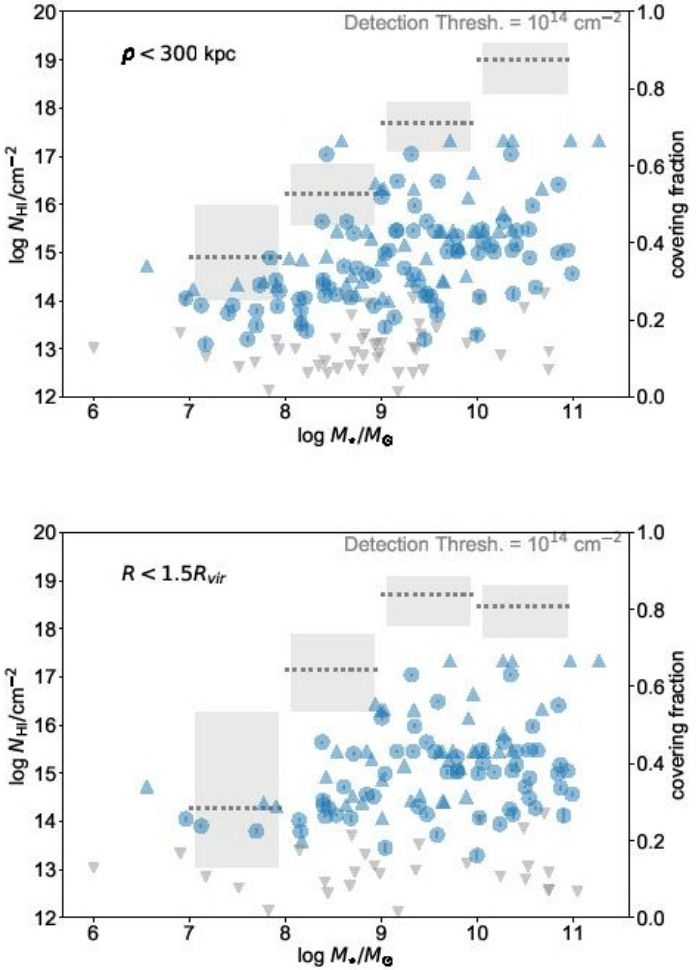

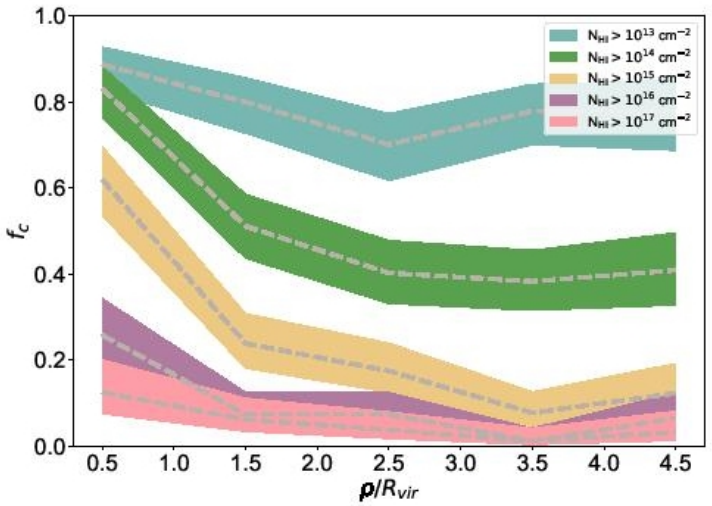

Figure 11. Covering fraction of H I as a function of $\rho/R_{\rm vir}$ for column density thresholds of $N_{\rm HI} > 10^{13}$ cm^{-2} (blue), $N_{\rm HI} > 10^{14}$ cm^{-2} (green), $N_{\rm HI} > 10^{15}$ cm^{-2} (yellow), $N_{\rm HI} > 10^{16}$ cm^{-2} (purple), and $N_{\rm HI} > 10^{17}$ cm^{-2} (pink). Shaded regions represent the 1-σ (68%) binomial confidence intervals. Here we connect the center of the radial bins to highlight the difference in the distributions. We see that for column densities less than 10^{14} cm^{-2} show little correlation with galaxies. The covering fraction at $R < R_{\rm vir}$ in for the highest column densities ($N_{\rm HI} > 10^{15}$ cm^{-2}) never gets higher than 0.7.

Плотный газ виден далеко за вириальный радиус

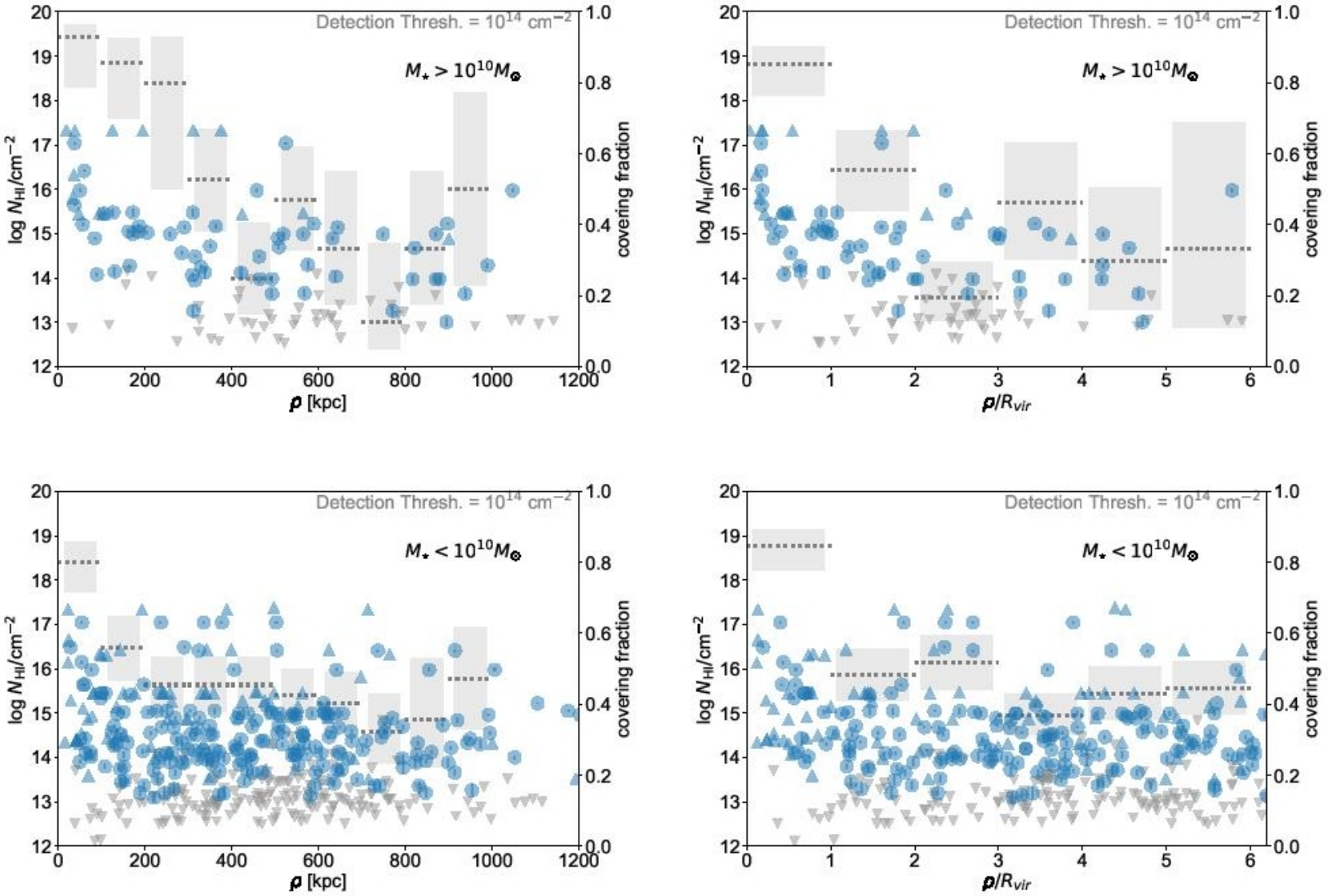

igure 10. Column density N_{HI} as a function of impact parameter, ρ (left) and R_{vir} (right). The top panels show galaxies

По скоростям он привязан к галактикам – особенно к массивным

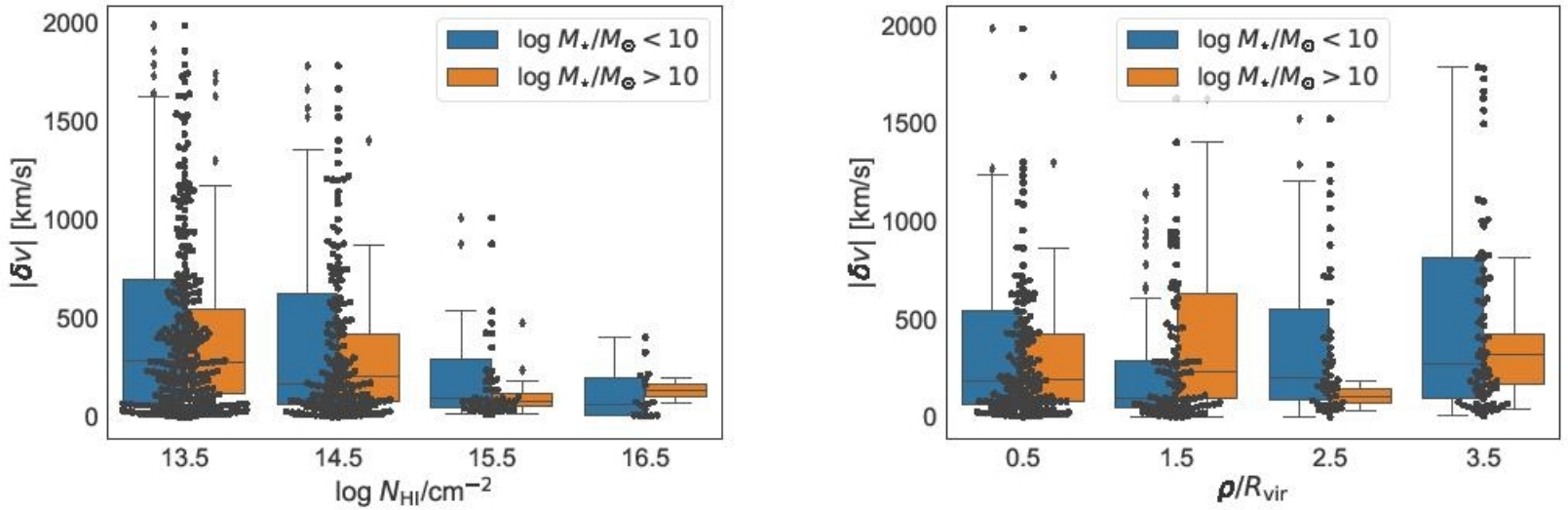

Figure 12. The distribution of absolute velocities as a function of $N_{\rm HI}$ and $\rho/R_{\rm vir}$ displayed in a box and whisker plot. The boxes display the quartiles of the distribution centered at each column density and radial bin while the whiskers extend to show the rest of the distribution of the bins. Outliers are defined as points that lie outside 1.5 times the innerquartile range and are displayed as diamonds. The black points on top of the box plots indicate the velocity of the of each absorption component in the corresponding bins. Each bin is split into a high (blue) and low-mass (orange) sample. We see a strong anticorrelation between velocity spread and column density. The component velocity centroids do not exhibit any clear trends with impact parameter.

Оценки средних размеров газовых дисков

5.3. *Estimating* $R^{14}_{\rm CGM}$

In order to estimate a characteristic size of the $N_{\rm HI} > 10^{14}$ cm^{-2} CGM, $R^{14}_{\rm CGM}$, we devise a method in which we use the parameters to calculate the impact parameter at which the covering fraction ($f_c = P^{\rm hit}$) exceeds 0.5. Within this impact parameter, a sightline has a greater than 50% chance of exhibiting a H I column with $N_{\rm HI} > 10^{14}{\rm cm}^{-2}$. We can then estimate the posterior distribution of $R_{\rm CGM}$ by calculating it for each sample taken from the posterior distributions of γ and r_0. In the high-mass sample, we determine $R^{14}_{\rm CGM,p} = 0.362^{+0.083}_{-0.072}$ in physical Mpc ($R^{14}_{\rm CGM,c} = 0.482^{+0.111}_{-0.096}$ comoving Mpc) and $R^{14}_{\rm CGM,p} = 0.281^{+0.042}_{-0.036}$ physical Mpc ($R^{14}_{\rm CGM,c} = 0.366^{+0.054}_{-0.047}$ comoving Mpc) for the low-mass sample. These correspond to $R^{14}_{\rm CGM} = 1.42^{+0.33}_{0.28}$ $R_{\rm vir}$ and $R^{14}_{\rm CGM} = 2.31^{+0.35}_{-0.30}$ $R_{\rm vir}$ for the high-and low-mass samples, respectively, where $R_{\rm vir}$ was calculated using the mean redshift and mass of each sample. These estimates are in agreement with our qualitative empirical estimates from the previous analysis.